Supplementary Materials: Impact of Deep Eutectic Solvents Impact on Kinetics and Folding Stability of Formate Dehydrogenase

Nicolás F. Gajardo-Parra [1], Gabriel Rodríguez [1], Andrés F. Arroyo-Avirama [2], Astrit Veliju [3], Thomas Happe [3], Roberto I. Canales [2], Gabriele Sadowski [1] and Christoph Held [1,*]

1. Supplementary Figures:

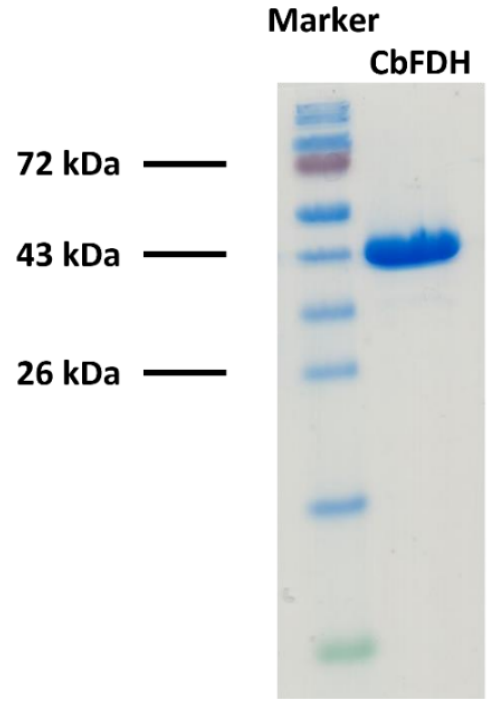

Figure S1. SDS-PAGE of purified *cb*FDH

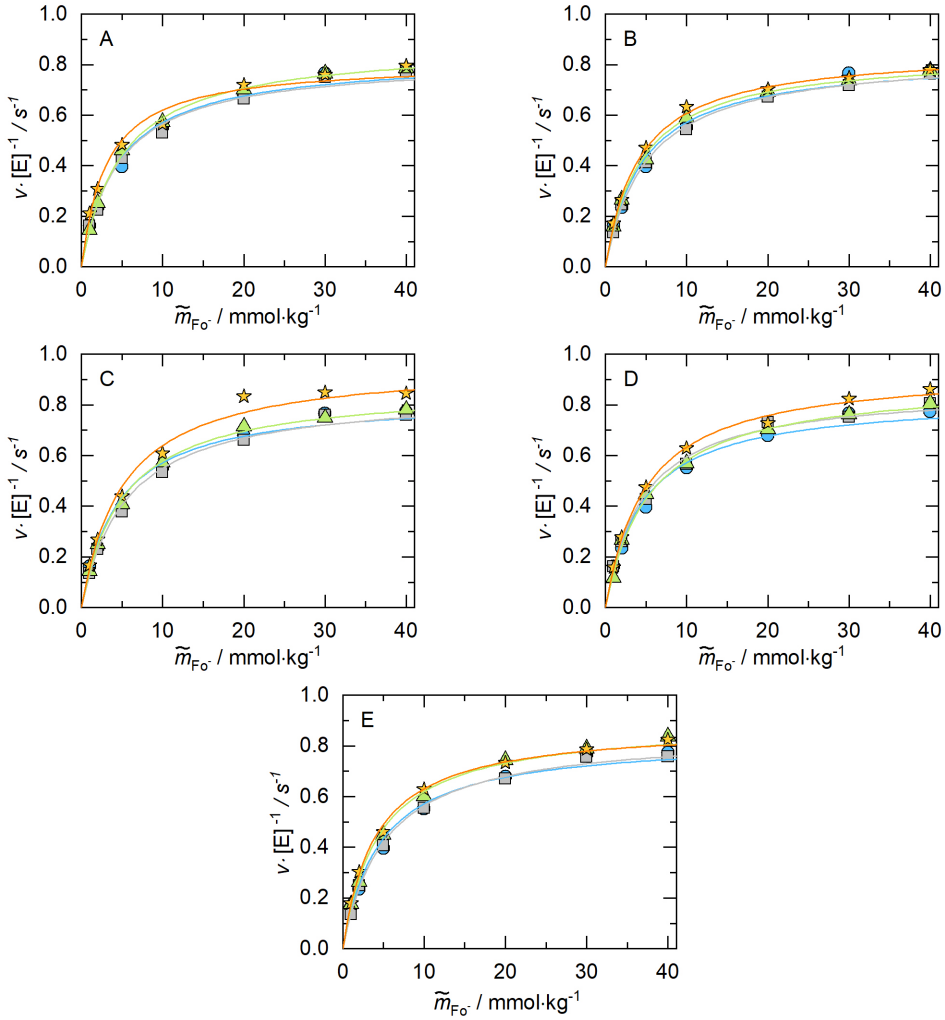

Figure S2. Michaelis-Menten curves for the *cb*FDH reaction (T = 25 °C, p = 1 bar) with various co-solvents (A: BET, B: GLY, C: SOR, D: DES1, E: DES2) at different concentrations (grey: 5 wt.-%, green: 10 wt.-%, orange: 15 wt.-%, blue: neat buffer). Here the reaction rate v normalized to the enzyme total molality is plotted against the formate molality.

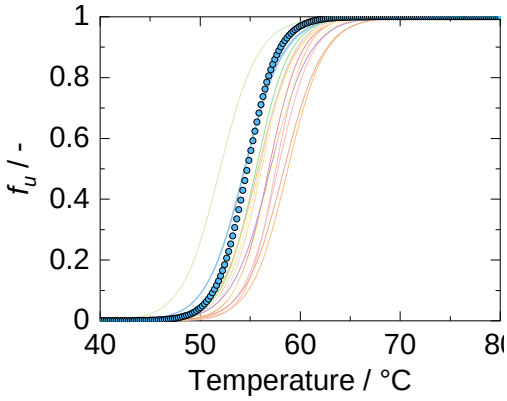

Figure S3. Sigmoidal curves of the fraction of unfolding cbFDH molecules as a function of the temperature obtained from fluorescence measurements via nanoDSF. Each system is represented by a different color, with the blue curve with circles describing the neat buffer.

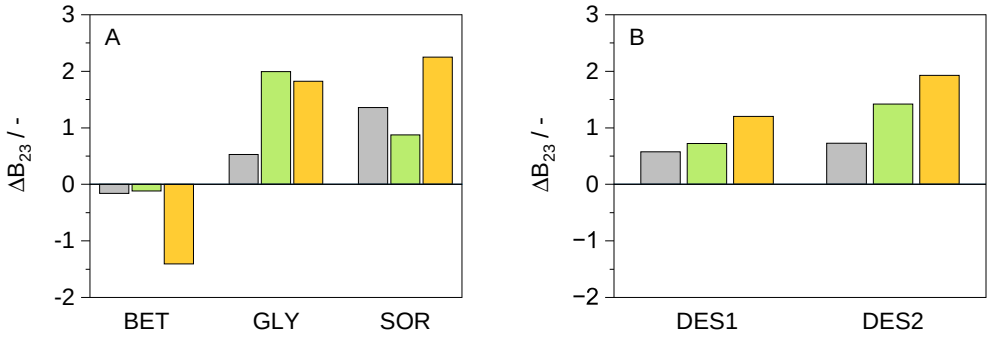

Figure S4. Graphical representation of the results obtained for the $\Delta B_{2,3}$ of *cb*FDH in the presence of various co-solvents (A: BET, GLY, SOR / B: DES1, DES2) at different concentrations (grey: 5 wt.-%, green: 10 wt.-%, orange: 15 wt.-%, value 0: neat buffer).

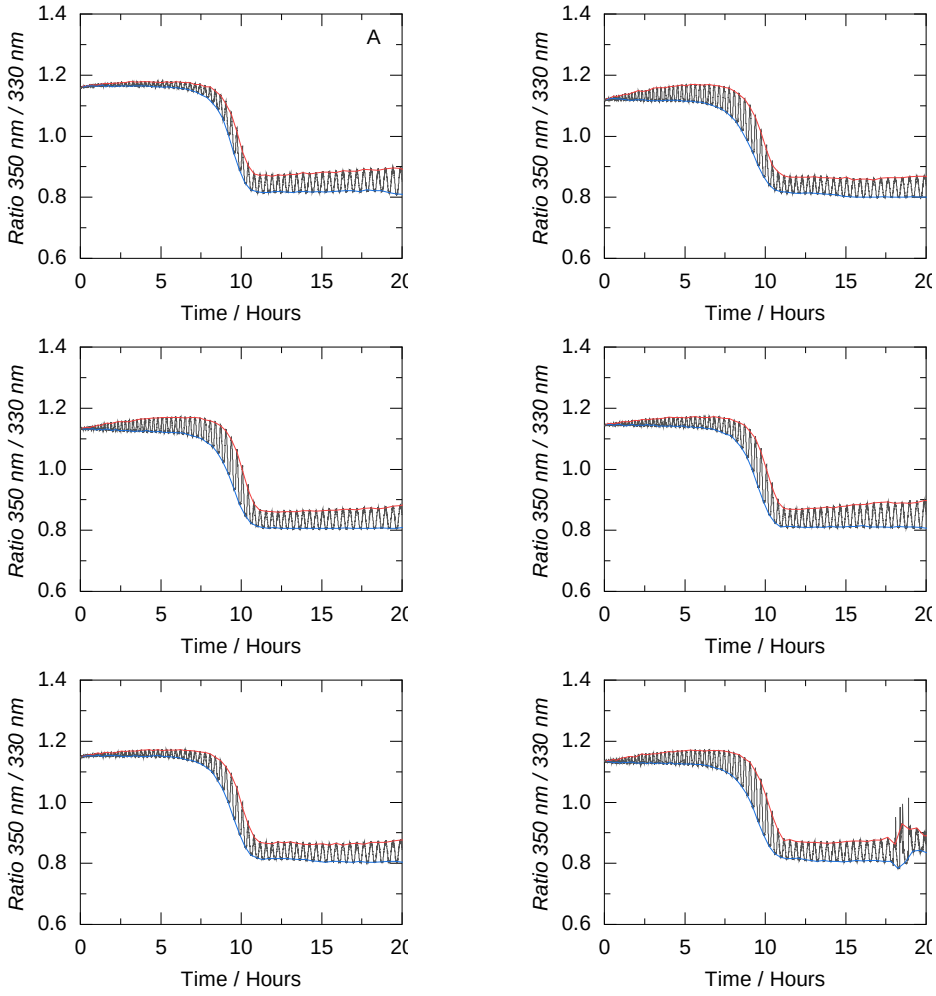

Figure S5. Unfolding (blue) and non-reversibility (red) curves of *cb*FDH obtained from the MSF measurements under the influence of various co-solvents at 5 wt.-% concentration (A: buffer, B: BET, C: GLY, D: SOR, E: DES1, F: DES2). Here the fluorescence ratio at 350 nm and 330 nm is plotted against the time. Its scale (x-axis) correlates to the temperature during the measurement (between 20-80 °C).

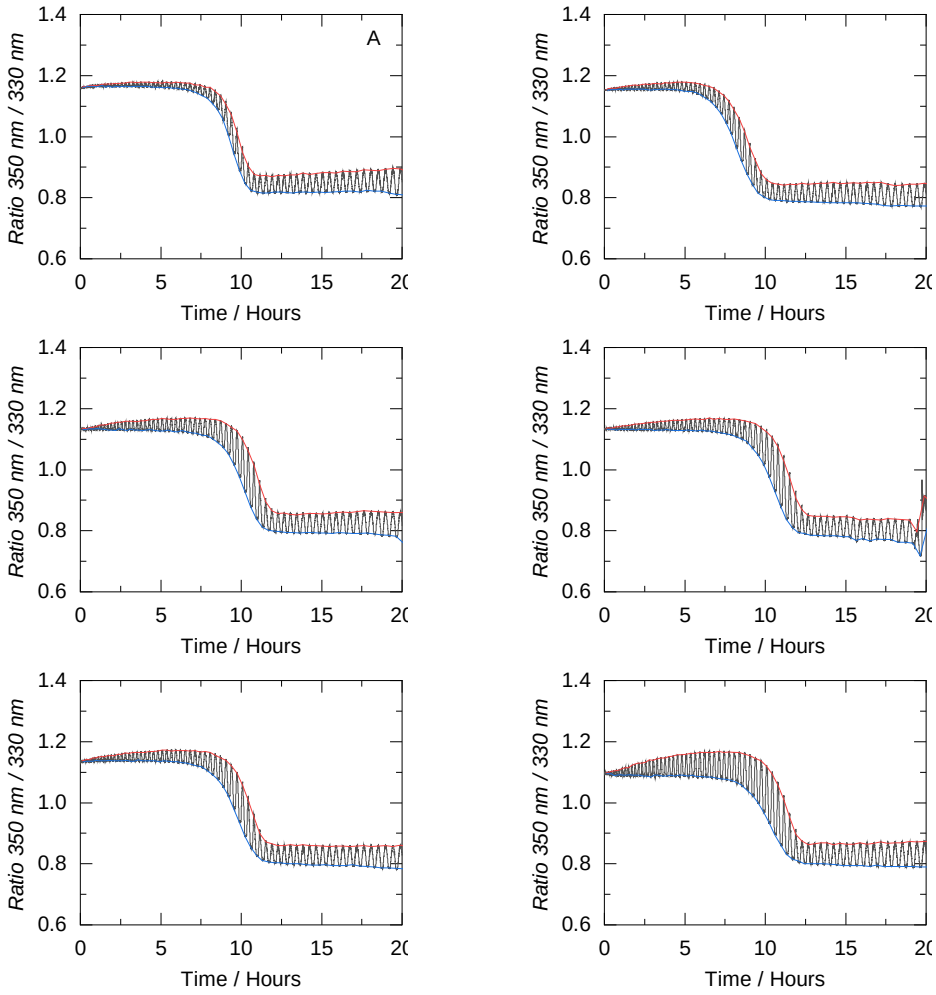

Figure S6. Unfolding (blue) and non-reversibility (red) curves of *cb*FDH obtained from the MSF measurements under the influence of various co-solvents at 15 wt.-% concentration (A: buffer, B: BET, C: GLY, D: SOR, E: DES1, F: DES2). Here the fluorescence ratio at 350 nm and 330 nm is plotted against the time. Its scale (x-axis) correlates to the temperature during the measurement (between 20-80 °C).

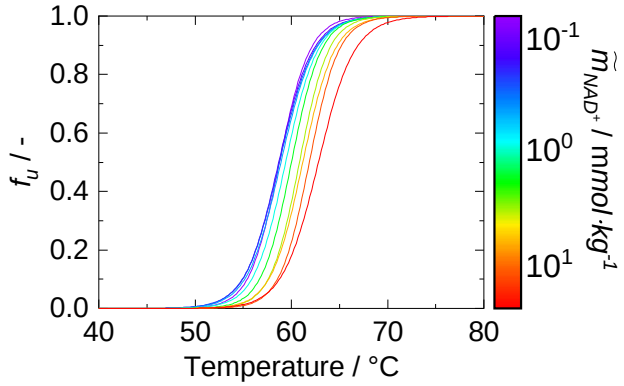

Figure S7. Qualitative illustration of the sigmoidal curves of the fraction of unfolding *cb*FDH molecules with bound NAD^+ as a function of the temperature, obtained from fluorescence measurements via nanoDSF. Each NAD^+ molality is shown in a color scale, with blue representing the lowest and red the highest.

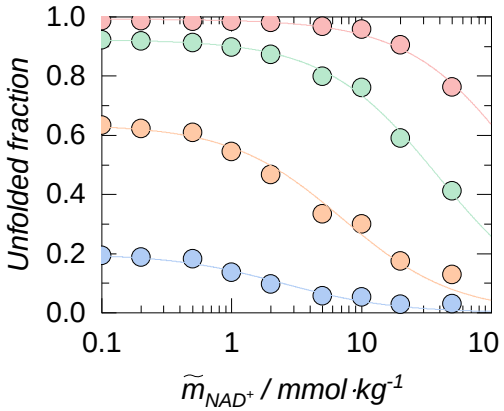

Figure S8. Qualitative illustration of the unfolding curves obtained from the isothermal approach using FoldAffinity as a function of the NAD^+ molality. Every curve was measured for a specific system at a different temperature in a range $T_u \pm 10$, with the red curve representing the highest temperature and the blue curve the lowest.

2. Supplementary Tables:

Table S1. List of the chemicals utilized in this work, including the compound name, the Chemical Abstracts Service (CAS) Number, the purity, and the supplier.

Compound	CAS-Number	Purity / wt.-%	Supplier
Formate dehydrogenase	obtained from recombinant *E.coli*		
Sodium formate	141-53-7	>99.0	VWR Chemicals
NAD^+	53-84-9	>96.5	Sigma-Aldrich
Betaine	107-43-7	>99.0	Sigma-Aldrich
Glycerol	56-81-5	>99.5	VWR Chemicals
D-Sorbitol	50-70-4	>99.0	Sigma-Aldrich
Trizma Base	77-86-1	>99.9	Sigma-Aldrich
Trizma Hydrochloride	1185-53-1	>99.0	Sigma-Aldrich

Table S2. Kinetic parameters (K_M, k_{cat} and K_{eff}) of the *cb*FDH reaction (T = 25 °C, p = 1 bar) under the influence of different co-solvents obtained from Equation 2.

System	$K_{M,formate}$ mmol·kg^{-1}	k_{cat} s^{-1}	K_{eff} kg·mmol^{-1}·s^{-1}
Buffer	5.488	0.884	0.161
5 wt.-% BET	5.505	0.874	0.159
10 wt.-% BET	5.02	0.884	0.176
15 wt.-% BET	3.933	0.863	0.22
5 wt.-% GLY	5.395	0.858	0.159
10 wt.-% GLY	4.71	0.862	0.183
15 wt.-% GLY	4.09	0.855	0.209
5 wt.-% SOR	6.083	0.883	0.145
10 wt.-% SOR	5.316	0.885	0.167
15 wt.-% SOR	5.287	0.98	0.185
5 wt.-% DES1	5.153	0.899	0.175
10 wt.-% DES1	5.808	0.917	0.158
15 wt.-% DES1	5.296	0.965	0.182
5 wt.-% DES2	5.402	0.868	0.161
10 wt.-% DES2	5.063	0.933	0.184
15 wt.-% DES2	4.392	0.907	0.207

Table S3. Thermal parameters (T_u, $\Delta\Delta G'_u$, B_{23}, $pk'^{o}{}_u$, and T_{eclu}) for *cb*FDH under the influence of various co-solvents at different concentrations. The results were obtained after data analysis via MoltenProt.

System	T_u °C	$\Delta\Delta G'_u$ kJ·mol^{-1}	ΔB_{23} -	$pk'^{o}{}_u$ -	T_{eucl} °C	T_{nr} °C	K_D mM
Buffer	54.71	0	0	8.381	72.69	58.9	1.55
5 wt.-% BET	54.41	-0.102	-0.157	7.034	71.15	58.8	0.807
10 wt.-% BET	54.48	-0.077	-0.119	6.918	71.17	58.8	0.978
15 wt.-% BET	52.00	-0.916	-1.407	6.472	67.77	56.2	1.69
5 wt.-% GLY	55.59	0.343	0.526	8.584	73.48	59.7	1.14
10 wt.-% GLY	57.57	1.298	1.994	8.772	76.94	61	1.103
15 wt.-% GLY	57.78	1.188	1.825	9.177	76.51	62.1	0.272
5 wt.-% SOR	56.87	0.883	1.356	8.885	75.5	59.8	0.537
10 wt.-% SOR	56.12	0.568	0.873	8.66	74.37	61.4	0.774
15 wt.-% SOR	58.77	1.465	2.25	8.906	77.54	63.3	1.02
5 wt.-% DES1	55.78	0.376	0.577	7.881	73.23	59.4	0.67
10 wt.-% DES1	55.93	0.471	0.723	7.818	73.91	60	0.794
15 wt.-% DES1	57.03	0.783	1.202	7.886	74.75	60.7	0.577
5 wt.-% DES2	56.02	0.473	0.726	8.02	73.71	60	0.22
10 wt.-% DES2	57.17	0.924	1.42	8.079	75.51	61.1	0.19
15 wt.-% DES2	58.40	1.257	1.93	7.695	76.7	62.8	0.176